Self-similarity of pressure profiles during forced granular flows

María Victoria Ferreyra,[1] Luis A. Pugnaloni [1,2] and Diego Maza [3,*]

[1]*Departamento de Física, Facultad de Ciencias Exactas y Naturales, Universidad Nacional de La Pampa, Uruguay 151, 6300 Santa Rosa, La Pampa, Argentina*
[2]*Consejo Nacional de Investigaciones Científicas y Técnicas, 2290 Godoy Cruz, Buenos Aires, Argentina*
[3]*Departamento de Física y Matemática Aplicada, Facultad de Ciencias, Universidad de Navarra, 31080 Pamplona, Spain*

We present measurements of the vertical stress profile σ on the base of flat-bottomed cylindrical silos discharged through an orifice centered on its base. An overweight forces the material on top of the free surface. The mean bottom pressure $\sigma(z, D, W)$, with z the height of the granular column, D the silo diameter, and W the mass of the overweight, increases significantly at the end of the discharge. Inspired by early models of stress distribution, we show that σ measured at $z = 0$ can be rescaled to yield a collapse of the data, as a function of z/D, for all D and W explored. We also show that the profile $\sigma(r)$ is self-similar as a function of the radial coordinate r and can be rescaled to collapse the data for different z, D, and W. Although the model correctly predicts the functional dependences, it fails in quantitative terms. These results challenge our understanding of free and forced granular flows through orifices.

Introduction. When a dense granular material flows under gravity through a constriction, some peculiar phenomena, when contrasted against inviscid fluids, become apparent [1]. Among them, the flow rate remains constant [2,3] (or slightly increases) while the containing vessel is emptied. This is often attributed to the also peculiar Janssen effect [1,4], which renders the bottom pressure of a static granular column in a vertical silo almost independent of the column height (if the height is above twice the container diameter). However, under flowing conditions, the bottom pressure and flow rate seem to be decoupled [5–11].

Walker [12] improved Janssen's model of the bottom pressure in a flowing silo by using the Coulomb yield criterion and the Mohr circle scheme to put Janssen's redirection factor K as a function of the internal angle of friction and the wall friction. Walters elaborated these ideas and included predictions for forced flows [13]. The main result of the Walker-Walters (WW) approach is that in the flowing regime, the pressure depends on a new parameter that replaces the well-known Janssen K factor. It is noteworthy that the pressure is not predicted to depend on the velocity of the flow. More than 30 years later, Bertho *et al.* [14] experimentally demonstrated that the pressure at the bottom of a cylindrical vertical tube for a moving column of grains is much more reproducible than for a static material (due to the well-defined dynamic friction force) and independent of the velocity over four orders of magnitude. This validates in part Walter's ideas, which were not recognized at the time. More recently, Windows-Yule *et al.* [15] have reproduced this finding numerically under more general flowing conditions, using laterally moving sidewalls.

To put models to the test, recent studies have explored the effect of forcing the granular flow via mechanisms additional to the weight of the granular material [16–19]. If an extra weight is added to the top of the granular column, the flow rate and the bottom pressure can be increased significantly, thus refuting some early predictions about the flow of forced granular flows [20]. The traditional free-fall arch approximation, which has been challenged [21] but leads to the well-known Beverloo equation [22], becomes hopeless in these systems since the flow rate does not remain constant during discharge. Recent approaches based on energy balance [23] may help in this respect. However, there is a lack of validated models and empirical relations for the scaling of pressure with silo diameter, column height, and external forcing.

In this Letter we present a series of experiments of forced silo discharge for a range of silo diameters and external forcing. We measure the evolution of the vertical pressure profile at the base of the silo using a capacitive sensor array. We show that the mean pressure is consistent with the WW model [13]. Significantly, the bottom pressure, irrespective of the forcing condition, can be collapsed into a single master curve when the column height is scaled with the silo diameter and the mean stress is normalized with the difference between the pressure exerted by the piston and the asymptotic pressure measured for a very tall granular column. The radial pressure profile measured at the silo bottom is nonuniform, which contradicts Walter's starting hypothesis and can be collapsed for the various z, D, and W. These collapses align with previously reported self-similarity properties in the silo discharge process [21,24].

Experimental setup. Silos are made of stainless-steel (0.5–1.5)-m-long cylindrical tubes of internal diameters $D = 0.048$, 0.056, 0.067, and 0.080 m. The base is separated from the walls and has a circular hole (diameter $D_0 = 0.014$ m)
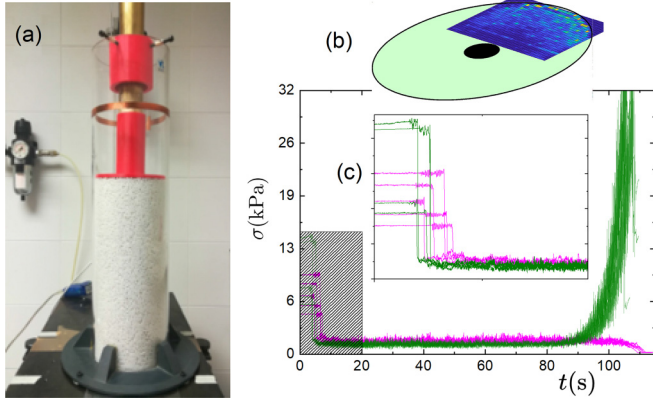
_____
*dmaza@unav.es

FIG. 1. (a) Photo of the experimental setup (we set a glass tube to make the material visible to the reader). (b) Snapshot of the capacitive sensor array response, including schematics of the silo base. (c) Mean normal pressure σ at the base ($D = 0.048$ m and the initial column height is 0.60 m) during discharge for free ($W = 0$ kg, pink) and forced ($W = 6.0$ kg, green) flow as a function of time. Five realizations are shown for each W. The inset shows a closeup of the shadow region.

FIG. 2. Mean bottom pressure σ as a function of z for (a) $D = 0.048$ m and different W and (b) $W = 6.0$ m and different D. (c) and (d) Same data as in (a) and (b) using rescaled pressures and rescaled column height [see Eq. (2)]. The solid line corresponds to Eq. (2) using $\beta = 0.168$ in both (c) and (d). The insets show the saturation pressure σ_∞ as a function of (c) W and (d) D. Error bars correspond to the standard deviation over realizations. The solid lines correspond to $\sigma_\infty = g\rho_b D/4\beta$ as predicted by Eq. (1).

at its center. Glass beads (material density $\rho = 2500$ kg/m³, Young's modulus $E = 70$ GPa, and diameter 2.0 ± 0.2 mm) are used as the granular material. Forcing is done using cylindrical pistons that fit in the corresponding tubes with a gap smaller than 1.0 mm [see Fig. 1(a)]. These pistons can have weights W up to 8.0 kg. The base and the vertical walls are separated by less than 1.0-mm spacers that leave a gap wide enough to fit a capacitive sensor array while preventing the glass beads from leaking through the gap. The sensor and base are taped to create a homogeneous leveled surface. The 250-μm-thick array sensor (Tekscan Pressure Mapping Sensor 5051-High sensitivity) consists of a square 44×44 matrix of sensors of 1.27×1.27 mm² each. This array is placed on the base of the silo and covers only part of the cross section, just reaching the edge of the central orifice [see Fig. 1(b)]. Sensors provide 256 pressure levels acquired at 100 samples per second. We adjusted the sensitivity of sensors to span the range of pressures observed in the experiments. Only a few sensors were observed to saturate for the highest pressures tested. The sensor has a different (smoothly nonlinear) response under static and dynamic conditions. We calibrated the taped sensor by dragging on top of it known weights supported by a layer of 2-mm glass particles at a low velocity (0.3 cm/s) compatible with the radial velocity of the grains during discharge. Details of the procedures used to calculate the mean pressure and pressure profiles can be found in the Supplemental Material [25]. An electronic balance (AND EK-4100i, 0.1 g, 10 Hz) beneath the silo records the total weight of grains poured and a proximity ultrasound sensor (Pasco PS-2103A, 1.0-mm precision, 50 Hz) on top of the silo measures the position of the top piston as a function of time. We confirmed that the column height and discharged mass are proportional to each other throughout the discharge corresponding to a constant bulk density ($\rho_B = 1590 \pm 20$ kg/m³).

Results. Figure 1(c) shows the mean normal pressure σ_{zz} on the base (we drop the subscript in the following) as a
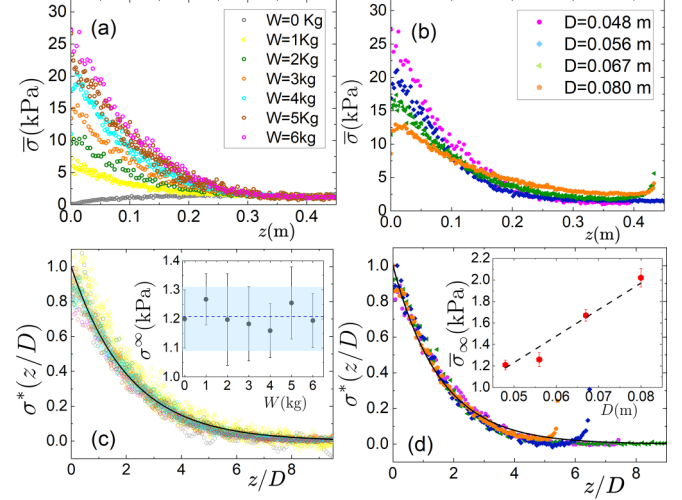
function of time during discharges made with and without overweight. After the filling process but before starting the discharge, σ shows constant plateaus with high variability between different realizations. However, as soon as the material flows, the stress rapidly evolves to the same value in all realizations. The dynamic pressure plateau is consistent with a dynamical Janssen effect [14,26–28] when the height of the material is large (we denote this value by σ_∞). However, σ increases significantly in the final stages of the discharge for $W = 6.0$ kg, in agreement with recent studies [16]. In the results reported below, averages over five independent realizations of the experiment are used. At the end of the discharge, when the height z of the granular column drops to zero, the pressure reaches σ_0, the pressure exerted by the piston alone ($\sigma_0 = 4Wg/\pi D^2$, with g the acceleration of gravity). In Figs. 2(a) and 2(b) we plot σ for various W and D as a function of the column height z. As expected, an increase of W or a decrease of D increases the pressure sooner (at higher z during discharge). Notably, the pressure plateau σ_∞ is the same for all the overweights explored but grows monotonically with the silo diameter.

The traditional Janssen theory writes the force balance on any horizontal slice of the material inside the silo. It assumes that (i) the z and r directions coincide with the principal stresses (Mohr's circle) and (ii) the stresses are uniform across the slice [2]. Then the shear stress at the wall is estimated as $\sigma_{rz}^w = \mu_w \sigma_{rr}$ (wall yield locus) and assumes the constitutive relation $\sigma_{rr} = K\sigma_{zz}$, with K the so-called Janssen distribution factor. Hence, $\sigma_{rz}^w = \beta\sigma_{zz}$ with $\beta = \mu_w K$. If the material is in the critical state of internal yield, then K can only take two possible values: If the z direction is the major principal stress, then we say that the system is in an active Rankine state and $K < 1$; if it is the minor principal stress we call

this a passive Rankine state and $K > 1$ [2]. The active state corresponds to the static conditions, whereas the passive state develops during discharge [2]. The WW model improves the analysis by considering that (i) the stresses are not uniform in the slice and (ii) the principal stresses at the wall form an angle ϵ with the z and r directions [12,13]. The expression obtained by Walker and Walters for the stress normal to the silo base filled up with grains to a height z and with an overweight of mass W for a discharging (passive Rankine state) column is [12,13]

$$\sigma(z) = \frac{g\rho_b D}{4\beta}(1 - e^{-4\beta z/D}) + \frac{4gW}{\pi D^2}e^{-4\beta z/D}, \qquad (1)$$

with β a corrected Janssen-like constant that is a function of the internal and wall friction angles (see [25] for details). The limits $z \to \infty$ and $z \to 0$ are $\sigma_\infty = \frac{g\rho_b D}{4\beta}$ and $\sigma_0 = \frac{4gW}{\pi D^2}$, respectively. In the insets of Figs. 2(c) and 2(d) we show the measured σ_∞ as a function of W and D, respectively. These plots confirm that the saturation pressure does not depend on W and is linear on D. Both data sets can be fitted independently according to $\sigma_\infty = \frac{g\rho_b D}{4\beta}$, giving $\beta = 0.168 \pm 0.02$.

Let us define a rescaled pressure $\sigma^*(z^*)$ as

$$\sigma^*(z^*) = \frac{\sigma(z) - \sigma_\infty}{\sigma_0 - \sigma_\infty} \Rightarrow \sigma^*(z^*) = e^{-4\beta z^*}, \qquad (2)$$

with $z^* = z/D$. As we can see, $\sigma^*(z^*)$ should be the same for experiments with different W and D according to the WW analysis. Figures 2(c) and 2(d) show σ^* for various D and W tested, where we calculate the theoretical values of σ_∞ and σ_0 setting $\beta = 0.168$, following the fits shown in the insets. The data collapses onto a single functional dependence as predicted by Eq. (2) with $\beta = 0.168$. These results confirm that a single parameter β controls the saturation pressure and defines the exponential growth scale under forced conditions. It is worth mentioning that the pressure is independent of the flow velocity, as shown by Bertho *et al.* [14]. Hence, using a different orifice diameter will not alter the pressure law.

We estimate the particle-wall dynamic friction coefficient as $\mu_d = 0.170 \pm 0.005$ and the internal friction as $\mu_{int} = 0.46 \pm 0.02$ (see the Supplemental Material [25]). The WW model predicts $\beta = 0.38$ for these values, more than twice the value we obtained by fitting the pressure data. Below we discuss the possible mechanisms behind this discrepancy.

It is known that the pressure on a flat-bottomed silo is not homogeneous in either static [29] or dynamic [8] conditions. Figures 3(a) and 3(b) show the pressure over different concentric rings as a function of z and Figs. 3(c) and 3(d) the radial pressure profiles for the smallest and the largest silos studied at different stages of the discharge when the same overpressure $\sigma_0 = 15.5$ kPa is applied. The profiles depend nonlinearly on r and grow on average as the discharge proceeds. The profiles show clear oscillations because sensors are smaller than the grain size and can capture some degree of layering in the radial direction. Significantly, all the profiles can be collapsed by rescaling r by the silo radius $D/2$ and the pressure by the maximum stress measured next to the wall [Fig. 3(e)]. This collapse also works for all W and D, not only for the same applied overpressure [see Fig. 3(e)]. Previous studies, without overweight, have found more complex profiles [8,29]. However, in those investigations, the size of each sensor was
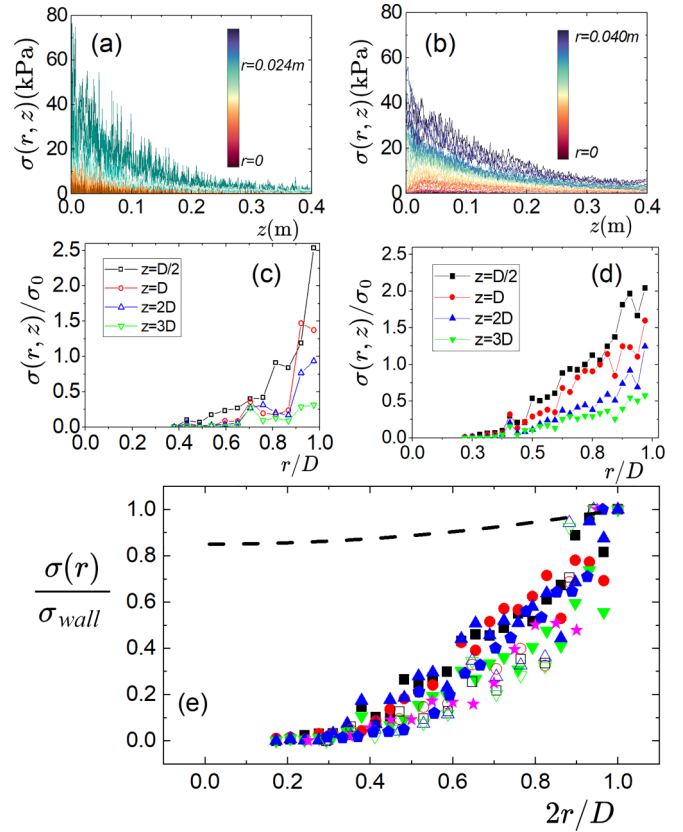

FIG. 3. (a) and (b) Bottom pressure as a function of z over different concentric rings (2.56 mm wide) for (a) $D = 0.048$ m and (b) $D = 0.080$ m with equal overpressure ($\sigma_0 = 15.5$ kPa). (c) and (d) Radial profiles of the normal pressure $\sigma(r)$ on the silo base for (c) $D = 0.048$ m and (d) $D = 0.080$ m at various column heights z during the discharge. (e) Pressure profile normalized by the maximum pressure σ_{wall} next to the silo wall as a function of rescaled radius [symbols are as in (c) and (d)]. We include data for $D = 0.056$ m (pink stars) and $D = 0.067$ m (blue pentagons) using an overweight $W = 8$ kg to show that the collapse works even if the forcing pressures differ. The dashed line corresponds to the Walters-Nedderman model [25].

larger than the particle size, and the grain size to silo diameter was significantly larger than in the present experiments. Walters and Nedderman made some attempts to extend Walters' calculations [30] and found a transcendental equation for the radial profile of the vertical stress [25]. Although the collapse in Fig. 3(e) aligns with the original assumptions used to derive β [12], the actual radial dependence of the model profile [dashed line in Fig. 3(e)] disagrees with the experiments. The Walters-Nedderman derivation does not consider the effect of the nearby orifice and should be valid only at a higher plane away from the silo base. Hence, the disagreement between the expected and fitted β values discussed above could be related to the region where we perform the measurements (next to the orifice). Moreover, Peralta *et al.* [31] showed that the material keeps memory of the filling protocol during a (not forced) silo discharge. Filling the silo with a hopper (as we do in this work), they obtained a Janssen-like factor $\beta = 0.155$. However, if the filling is distributed (rainlike), β becomes 0.35 (similar to the WW prediction above). One may speculate

that a sequential protocol homogenizes the stress distribution, making the WW approximations more suitable.

Conclusion. We have shown that the average normal pressure at the base of a forced discharging silo is consistent with the WW analysis [13]. Accordingly, the average stress can be collapsed into a single master curve using three parameters defining the problem scales, i.e., the silo diameter, the forcing overweight, and the Janssen-like β parameter [28]. Importantly, β depends not only on the internal friction but also on the material-wall friction. Radial pressure profiles are self-similar during discharge when normalized by the maximum pressure (next to the wall) for all silo diameters, forcing conditions, and column heights. More than ten years ago, Janda *et al.* demonstrated that the velocity and density profiles during free silo discharge are self-similar [24] and later Rubio-Largo *et al.* showed numerically that the vertical kinetic stress is self-similar too [21]. The present results generalize these ideas by demonstrating that the stress across the silo base is self-similar and is governed by a single scale, even in a forced (time-dependent) discharge regime.

The value of β obtained from the experiments deviates from the WW prediction. The disagreement seems to be caused by simplifications such as not accounting for memory effects and/or the presence of the orifice. Our result poses a challenge for developing a general model to predict granular flow and stress field, including forced systems. Recent approaches, like the local [32] and nonlocal [33] $\mu(I)$ rheology, could be particularly helpful in future developments.

[1] J. Duran, *Sands, Powders, and Grains: An Introduction to the Physics of Granular Materials* (Springer Science + Business Media, New York, 2012).

[2] R. M. Nedderman, *Statics and Kinematics of Granular Materials* (Cambridge University Press, Cambridge, 2005).

[3] J. Koivisto and D. J. Durian, Nat. Commun. **8**, 15551 (2017).

[4] H. A. Janssen, Z. Ver. Dtsch. Ing. **39**, 1045 (1895) [M. Sperl, Granul. Matter **8**, 59 (2006)].

[5] Z. Zhong, J. Y. Ooi, and J. M. Rotter, Eng. Struct. **23**, 756 (2001).

[6] H. Pacheco-Martínez, H. J. van Gerner, and J. C. Ruiz-Suárez, Phys. Rev. E **77**, 021303 (2008).

[7] M. A. Aguirre, J. G. Grande, A. Calvo, L. A. Pugnaloni, and J.-C. Géminard, Phys. Rev. Lett. **104**, 238002 (2010).

[8] C. Perge, M. A. Aguirre, P. A. Gago, L. A. Pugnaloni, D. Le Tourneau and J.-C. Géminard, Phys. Rev. E **85**, 021303 (2012)

[9] H. Ahn, Z. Başaranoğlu, M. Yılmaz, A. Buğutekin, and M. Z. Gül, Powder Technol. **186**, 65 (2008).

[10] M. A. Aguirre, J. G. Grande, A. Calvo, L. A. Pugnaloni, and J. C. Géminard, Phys. Rev. E **83**, 061305 (2011).

[11] L. Staron, P.-Y. Lagrée, and S. Popinet, Phys. Fluids **24**, 103301 (2012).

[12] D. M. Walker, Chem. Eng. Sci. **21**, 975 (1966).

[13] J. K. Walters, Chem. Eng. Sci. **28**, 13 (1973).

[14] Y. Bertho, F. Giorgiutti-Dauphiné, and J.-P. Hulin, Phys. Rev. Lett. **90**, 144301 (2003).

[15] C. R. K. Windows-Yule, S. Mühlbauer, L. A. Torres Cisneros, P. Nair, V. Marzulli, and T. Pöschel, Phys. Rev. E **100**, 022902 (2019).

[16] M. A. Madrid, J. R. Darias, and L. A. Pugnaloni, Europhys. Lett. **123**, 14004 (2018).

[17] M. A. Madrid and L. A. Pugnaloni, Granul. Matter **21**, 76 (2019).

[18] Z. Peng, J. Zhou, J. Zhou, Y. Miao, L. Cheng, Y. Jiang, and M. Hou, Phys. Fluids **33**, 043313 (2021).

[19] J. Horabik, P. Parafiniuk, J. Wiacek, R. Kobylka, M. Molenda, and M. Stasiak, Powder Technol. **403**, 117402 (2022).

[20] R. M. Nedderman, *Statics and Kinematics of Granular Materials* (Ref. [2]), Sec. 10.4.

[21] S. M. Rubio-Largo, A. Janda, D. Maza, I. Zuriguel, and R. C. Hidalgo, Phys. Rev. Lett. **114**, 238002 (2015).

[22] W. Beverloo, H. Leniger, and J. van de Velde, Chem. Eng. Sci. **15**, 260 (1961).

[23] J. R. Darias, M. A. Madrid, and L. A. Pugnaloni, Phys. Rev. E **101**, 052905 (2020).

[24] A. Janda, I. Zuriguel, and D. Maza, Phys. Rev. Lett. **108**, 248001 (2012).

[25] See Supplemental Material at http://link.aps.org/supplemental/10.1103/PhysRevE.109.L012901 for the sensor calibration protocol and internal angle estimation, details of the averaging protocols to calculate mean pressure and pressure profiles from the sensor array, and a brief review of Walters' model.

[26] L. Vanel and E. Clément, Eur. Phys. J. B **11**, 525 (1999).

[27] L. Vanel, P. Claudin, J.-P. Bouchaud, M. E. Cates, E. Clément, and J. P. Wittmer, Phys. Rev. Lett. **84**, 1439 (2000).

[28] G. H. L. Hagen, Ber. Bekanntmach. Geeigneten Verhand. Konigl. Preuss. Akad. Wiss. Berlin **17** 35 (1852) [B. P. Tighe and M. Sperl, Granul. Matter **9**, 141 (2007)].

[29] Y.-Y. Liu, D.-L. Zhang, B.-B. Dai, J. Su, Y. Li, and A. T. Yeung, Powder Technol. **381**, 601 (2021).

[30] J. K. Walters and R. M. Nedderman, Chem. Eng. Sci. **28**, 1907 (1973).

[31] J. P. Peralta, M. A. Aguirre, J.-C. Géminard, and L. A. Pugnaloni, Powder Technol. **311**, 265-272 (2017).

[32] L. Staron, P. Y. Lagrée, and S. Popinet, Eur. Phys. J. E **37**, 5 (2014).

[33] M. Bouzid, A. Izzet, M. Trulsson, E. Clément, P. Claudin, and B. Andreotti, Eur. Phys. J. E **38**, 125 (2015).